OXFORD

Institute of Chartered Foresters

Forestry: An International Journal of Forest Research, 2024, 1–13

https://doi.org/10.1093/forestry/cpae058

Original Article

Quantifying architectural uniqueness of Scots pine trees using terrestrial laser scanning: toward individual tree fingerprinting

Tuomas Yrttimaa[1,2,*], Samuli Junttila[1], Juha Hyyppä[3], Markus Holopainen[2,3], Michael A. Wulder[4], Mikko Vastaranta[1]

[1]School of Forest Sciences, University of Eastern Finland, P.O. Box 111, 80101 Joensuu, Finland
[2]Department of Forest Sciences, University of Helsinki, Latokartanonkaari 7, FI-00790 Helsinki, Finland
[3]Department of Photogrammetry and Remote Sensing, Finnish Geospatial Research Institute, National Land Survey of Finland, Vuorimiehentie 5, FI-02150 Espoo, Finland
[4]Canadian Forest Service, Natural Resources Canada, 506 Burnside Road West, Victoria, BC V8Z 1M5, Canada
*Corresponding author. E-mail: tuomas.yrttimaa@uef.fi

Abstract

Tree architecture reflects a hierarchical growth pattern shaped by the interplay between genetics and the environment. Environmental variation leads to unique resource availability, resulting in each tree developing distinct structural features, akin to the uniqueness of a human fingerprint. In this study, we propose a nondestructive method for quantifying this architectural uniqueness using terrestrial laser scanning for tree identification. While tree identification is commonly based on their precise geospatial location, this information may not always be available. Instead, we hypothesized that a tree's stem profile (diameters along the stem) and branching arrangement (locations of branch origins on the stem surface) could distinguish individuals within a population. The experimental setup included 65 Scots pine (*Pinus sylvestris* L.) trees in a managed boreal forest stand, scanned with terrestrial laser scanning in September 2021 (T1) and November 2022 (T2). We investigated whether individual trees could be identified based on architectural similarities between their point cloud reconstructions from T1 and T2. In total, 52 trees (80.0%) were identified based on their architectural characteristics. The results supported our hypothesis, showing that identifying ≥10 branch origins from independent reconstructions was sufficient to establish architectural uniqueness, resulting in 100% identification accuracy ($n = 20$ trees). These findings suggest that the complex three-dimensional tree architecture can be condensed into a two-dimensional pattern of points representing branch arrangement, which we term the "tree fingerprint." These architectural characteristics, which can be reconstructed from the lower half of the tree, are well suited for acquisition via ground-based sensing techniques such as terrestrial or mobile laser scanning. If point cloud data capable of characterizing individual branches is acquired during forest operations, the proposed methodology can facilitate tree identification for applications such as wood tracking, even without geospatial coordinates.

Keywords: close-range sensing; Lidar; tree identification; wood tracking; tree architecture

Introduction

Trees are the largest and most significant providers of ecosystem services in terrestrial ecosystems (Gamfeldt et al. 2013). They play a key role in the global carbon cycle, provide habitats for a large number of species, and offer economic value to communities and nations (Pregitzer and Euskirchen, 2004; Pan et al. 2011). While forest ecosystems harbor a variety of sites for trees to grow, no site is identical to others regarding resource availability. Even within the same geographical region and similar soil and climatic conditions, competition between individuals eventually regulates the availability of growth resources such as light, nutrients, and water. Tree architecture is a realization of the growth process, reflecting the interplay between genetics and the environment (Valladares and Niinemets, 2007). Tree architecture refers to the dimensions and spatial arrangement of its organs: stem, branches, and foliage (Reinhardt and Kuhlemeier, 2002) that determine the domain and the extent of biophysical processes such as photosynthesis (Enquist et al. 2009, Rosell et al. 2009). Tree clones sharing the same genotype and growing in close proximity will exhibit different phenotypes due to their interaction with one another and the environment (Callaway et al. 2003). This suggests that each tree develops a unique architecture, and, if this architecture can be consistently measured, it may allow for the distinction and identification of individual trees.

Tree architecture is shaped by the growth process generally driven by the availability of growth resources (Larson, 1969; Oliver and Larson 1996). The availability of these resources is controlled by the tree's adaptation to the environment and the interaction with other tree individuals in close proximity (Waring and Running, 2010). The growth process consists of two components: primary growth, which increases the length of the leading shoots and branches, and secondary growth, which increases the thickness of the stem and branches (Taiz and Zeiger, 2010). With limited availability, resources are allocated according to the priority theory, where respiration and primary growth are favored over secondary growth (Kobe and Coates, 1997). This means that

Handling editor: Fabian Fassnacht
Received 29 May 2024; **revised** 19 November 2024; **accepted** 21 November 2024

the allometric relationships within tree architecture reveal past growth conditions. For example, increased competition for sunlight drives a tree to enhance its light-capturing capacity by extending its foliage toward open spaces, prioritizing either vertical height growth or horizontal crown expansion (Gillet, 2008). The proportion of foliage not receiving sufficient amounts of sunlight cannot contribute to photosynthesis anymore, leading to the decline and the death of respective branches, causing crown asymmetry, resource allocation to maintaining living foliage (Taiz and Zeiger, 2010), with fewer resources being allocated to increase the thickness of the stem and branches.

Currently, it is understood that each tree is structurally unique as no two trees grow under the exact same environmental conditions (e.g. Larson 1969, Brousseau et al. 2013). Despite this understanding, there remains a need for quantitative studies to support this theory empirically. The main challenge has been finding ways to describe tree architectures to distinguish one tree from another precisely. However, state-of-the-art close-range sensing techniques could provide a solution (Disney et al. 2018, Malhi et al. 2018). Terrestrial laser scanning (TLS) has a demonstrated capacity for detailed tree characterization as it enables a millimeter level of geometric accuracy in the reconstruction of the three-dimensional (3D) structure of trees (Hackenberg et al. 2014). This 3D reconstruction of trees includes the characterization of the stem (e.g. Simonse et al. 2003; Liang et al. 2013) and crown dimensions (e.g. Henning and Radtke 2006; Ritter and Nothdurft 2018), foliage properties (e.g. Béland et al. 2011; Van der Zande et al. 2011), and branching structure (e.g. Åkerblom et al. 2017; Demol et al. 2022).

Detailed 3D observations can also be repeated over time, capturing structural changes in tree architecture (Srinivasan et al. 2014; Bogdanovich et al. 2021; Luoma et al. 2021). While TLS can provide geometrically accurate 3D models of specific objects, there is a concurrent need for computational techniques to extract meaningful information from the resulting point cloud data. Typically, this involves a semantic classification step to categorize each point based on its origin or the structure it represents, such as stem, branches, and foliage in the case of trees (e.g. Morsdorf et al. 2018, Xi et al. 2020). Once relevant structures of interest (e.g. branches with live foliage) have been identified, their properties can be analyzed or inferred from the respective point cloud reconstruction (Yrttimaa et al. 2020, Yrttimaa et al. 2023a). Ultimately, the effectiveness of capturing detailed tree architecture relies on the quality of the initial 3D reconstruction generated by the TLS and the sophistication of computational methods employed to discern and detail the identified structures from the point clouds.

Identification of individuals within a population requires that each member has unique qualities or features that make them recognizable from one another (Jain et al. 2007). Accurate identification of individuals also necessitates that these identifying features exist across the entire population, can be quantitatively and noninvasively characterized, and are sufficiently invariant over a period of time (Rai et al. 2020). For instance, the identification of people typically relies on biometric recognition through unique physical or behavioral traits, including fingerprints, iris patterns, facial features, voice, and signatures (Jain et al. 2007). Similarly, identifying individual trees hinges on their distinctive, measurable architectural characteristics. A digital twin of each tree individual can be captured using close-range sensing techniques, enabling the reconstruction and characterization of its architecture nondestructively (Calders et al. 2020). Based on an understanding of tree morphology, trees typically feature a main stem serving as the origin of branches. Usually, the stem surface cannot be reconstructed up to the treetop due to limited visibility through the occluding foliage (Liang et al. 2016), suggesting that the origins of branches on the stem surface could only be detected for the part of the stem that can be reconstructed from the point clouds (Yrttimaa et al. 2023a). Once detected, the locations of branch origins on the stem surface can be presented with respect to height above the ground and azimuth angle around the stem. This comprises a two-dimensional (2D) point pattern that can be derived for all tree individuals using detailed point clouds. It also remains relatively unchanged in time for live and dead, unpruned branches at the lower part of the stem. Due to the contribution of both environment and genetics to the phenotype of a tree individual, the branching arrangement is expected to vary among individuals to such an extent that it could serve as a distinguishing feature for identifying tree individuals.

In this study, we aim to provide empirical support for the uniqueness of tree structures and introduce a computational method for quantifying this trait. We explore this concept through an experimental framework involving a managed boreal forest stand of 65 Scots pine (*Pinus sylvestris* L.) trees, all subject to seemingly similar growing conditions and management history. Using bitemporal TLS, we characterize each tree's branching arrangement at two consecutive time points to investigate whether these arrangements can be consistently characterized from independent TLS acquisitions at such accuracy that enables the identification of individuals. This approach will provide insights into structural uniqueness, suggesting its potential for tree identification in situations where accurate geospatial positioning is not possible. We hypothesize that independent TLS reconstructions can distinguish individual trees based on their architectural characteristics, particularly the spatial relationship of their branching patterns. Additionally, we aim to determine the minimum set of branch origins required to define a tree's unique structure and evaluate the role of stem profile in this uniqueness. Based on the findings of these experiments, we provide emphasis toward utilizing this information for tree identification, beneficial to applications such as wood tracking.

Materials and Methods

Experimental design

The study site is a managed Scots pine–dominated forest stand of ~0.4 ha in size in Evo, southern Finland (61°11' N, 25°8' E), within the southern boreal forest biome. Typical to such forest stands that were regenerated by planting or seeding and managed by harvesting, the trees were approximately of the same age, ~50 years, and featured limited variation in their dimensions. According to the field inventory data acquired in 2021, the forest stand featured a mean density of 430 trees per hectare, a mean basal area of 23.8 m^2 per hectare, and basal area-weighted mean diameter and height of 28.2 and 22.8 m, respectively.

Terrestrial laser scanning data acquisition

Multiscan TLS data were acquired at two time points using different scanners and scan positions, resulting in slightly different 3D reconstructions of the trees (Table 1, Fig. 1). This approach was chosen to mimic realistic conditions, as acquiring data with an identical setup is often impractical in real-world applications. The trees were scanned for the first time on 2–3 September 2021 (T1) using a Leica RTC360 time-of-flight laser scanner, with a scanning setup consisting of 25 individual scan positions arranged in a regular grid of 16 m spacing across the forest stand. The

Table 1. Summary of the bitemporal terrestrial laser scanning data acquisition setup used to obtain 3D reconstruction of the studied trees at two time points, T1 and T2

	T1	T2
Acquisition date	2–3 September 2021	16 November 2022
Scanner type	Leica RTC360, time-of-flight	Riegl VZ-400i, time of flight
Field of view	310° vertical, 360° horizontal	100° vertical, 360° horizontal
Wavelength	1550 nm	1550 nm
Angular resolution	0.034°	0.04°
Beam divergence	0.5 mrad @ $1/e^2$	0.35 mrad @ $1/e^2$
Point spacing	3 mm @ 10 m distance	3.5 mm @ 10 m distance
Scanning geometry	25 scans, average of 16 m apart, coverage of 162 m^2/scan	23 scans, average of 11 m apart, coverage of 129 m^2/scan

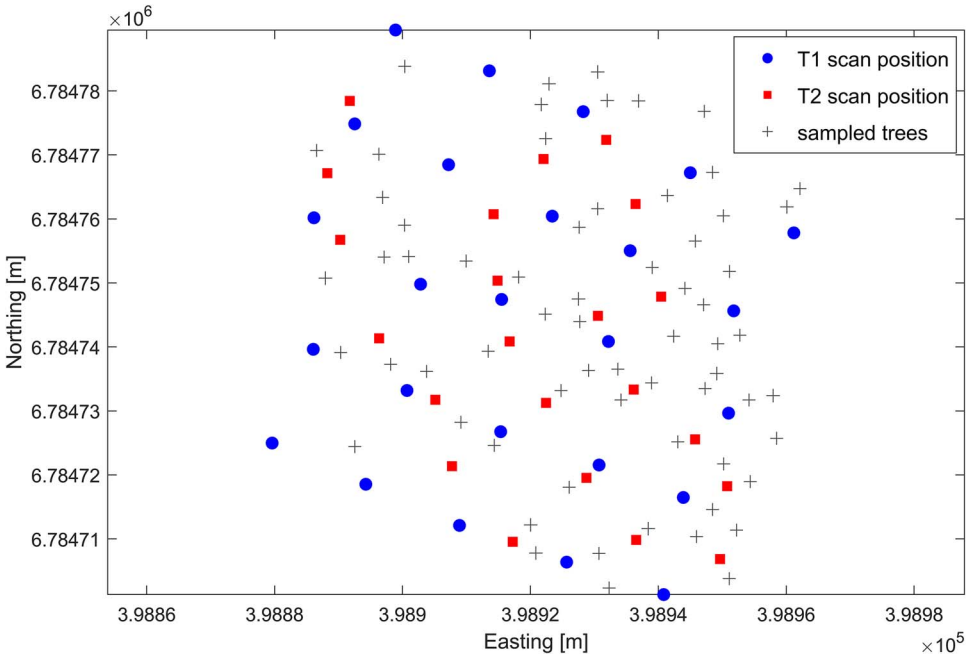

Figure 1. Illustration of the scanning geometries applied during the terrestrial laser scanning data acquisitions in September 2021 (T1) and November 2022 (T2). The figure shows the relative positions of the scan locations and their arrangement with respect to the studied trees, highlighting differences between the two acquisition campaigns.

scanner operated at a 1550 nm wavelength and a pulse repetition rate of 2000 kHz, delivering a hemispherical point cloud with a 300° vertical and a 360° horizontal field of view and an angular resolution of 0.034° resulting in a point spacing of 3 mm at a 10 m distance. All the scans were coregistered and merged using the Leica Cyclone Register360 software with artificial reference targets attached to trees. The co-existence of these known objects within point clouds acquired from different scan locations was utilized in determining rotation along the Z-axis and translation on the (X,Y) plane to align the point clouds with respect to each other.

The TLS campaign was repeated on 16 November 2022 (T2) using a Riegl VZ-400i (Riegl Laser Measurement Systems GmbH, Austria) time-of-flight terrestrial laser scanner operating at a 1550 nm wavelength and providing 100° vertical and 360° horizontal field of view. The scanner was operated at a pulse repetition rate of 600 kHz, which enabled recording up to eight returns per emitted laser pulse. The applied "Panorama 40" scan pattern featured an angular resolution of 0.04° and a point spacing of 3.5 mm at a 10 m distance. The multiscan setup consisted of 23 scans distributed around the forest stand, favoring locations with direct visibility to the treetops, considering the 100° vertical field of view of the scanner. While acquiring the scan data, the scanner provided automatic pose estimation based on built-in GNSS (global navigation satellite system) and IMU (inertial measurement unit) sensors. This enables automatic on-board coregistration of the individual scans without the use of external reference targets. The raw scan data from individual scans were converted to point clouds that were coregistered and merged in the RiSCAN PRO processing software (version 2.14.1) provided by the scanner manufacturer.

Point cloud preprocessing and semantic classification

The acquired point clouds were delineated according to the extent of the study area and thinned to a regular point spacing of 1 mm. A standard height-normalization procedure was applied separately for T1 and T2 point clouds to remove topography from the point clouds following the workflow presented by Ritter et al. (2017). Individual trees were then segmented from the point clouds using marker-controlled watershed segmentation (Yrttimaa et al. 2020; Popescu and Wynne, 2004). During this process, the tops of the 10 tallest trees were identified from both the T1 and T2 point

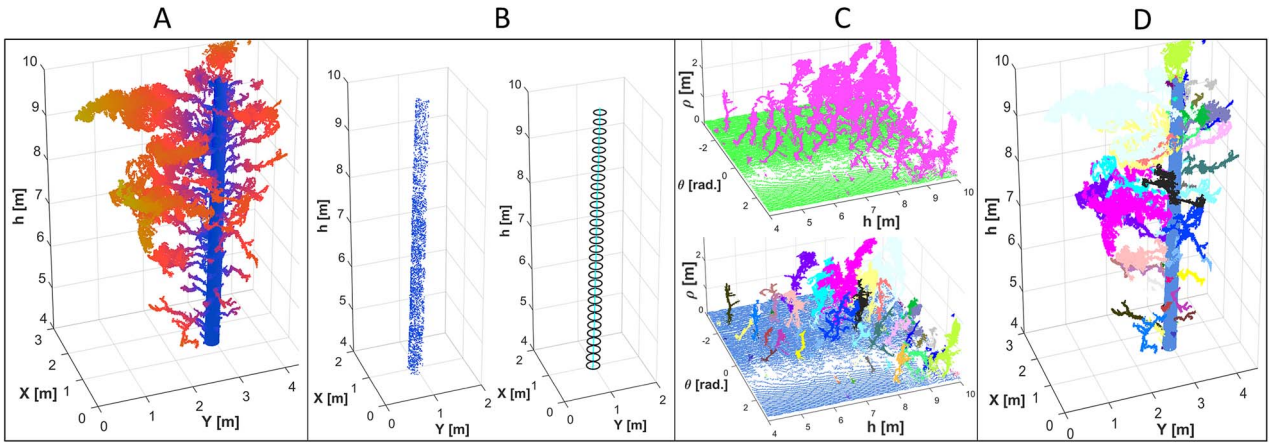

Figure 2. Semantic point cloud classification method for identifying stems and branches. Points from smooth, vertical, and cylindrical surfaces were considered as candidate stem points to determine stem orientation (A, B). The point cloud was converted from 3D cartesian (X,Y,*h*) to cylindrical coordinates (θ,*ρ*,*h*), where branch points showed variation in *ρ*, allowing separation of stem and branches (C). The obtained classification labelling was then applied to the original point cloud in Cartesian coordinates (D).

clouds. Their (X,Y) coordinate pairs were used to compute a rigid 2D transformation, including *XY* translation and *Z*-axis rotation, to align the T1 point cloud (in local coordinates) with the T2 point cloud (in global coordinates). A point-in-polygon approach was then applied to extract individual tree point clouds at T1 and T2. In closed canopy conditions, these point cloud segments could represent the crowns of multiple trees. Trees were automatically further delineated from each other if multiple stems were found within the point cloud segment (see Yrttimaa et al. 2020).

For each individual tree point cloud, a semantic classification method was then applied at both T1 and T2 to identify points originating from the stem surface (i.e. "stem points") following a procedure initially presented by Yrttimaa et al. (2023a) (Fig. 2). The classification employed a coordinate conversion from 3D Cartesian (X,Y,Z) to 3D cylinder representation (θ,*ρ*,*h*), where the location of each point was defined as an azimuth angle (θ) and radius (*ρ*) with respect to a stem orientation axis at a given height (*h*). With the cylinder representation, it was assumed that the stem points would spread on a 2D plane defined by θ and *h*, featuring a low variation in the *ρ*-coordinates. Respectively, points originating from branches and foliage would seemingly deviate from the (θ,*h*)-plane, featuring a higher variation in the *ρ*-coordinate than the stem points (Fig. 2C).

To complete the conversion, information on stem orientation was first obtained based on candidate stem points featuring smooth, vertical, and cylindrical neighborhoods. Least-squares circle fitting and linear interpolation were applied to obtain a stem orientation curve representing the midpoint of the stem cross-section as a function of height (Fig. 2A and B). The coordinate conversion was then carried out for each point by computing *ρ* as the horizontal Euclidean distance to stem orientation axis, θ as the four-quadrant inverse tangent (atan2) based on the X and Y components of the obtained *ρ*, while *h* equaled Z (Yrttimaa et al. 2023a). Coordinate conversion from 3D Cartesian into 3D cylinder representation made the stem points appear on a flat surface aligning with the (θ,*h*)-plane, while points originating from branches and foliage (i.e. "branch points") were forming clusters deviating from that surface (Fig. 2C). This setup allowed us to separate stem points from branch points using a simple morphological filter algorithm (Pingel et al. 2013). The procedure resembled identifying terrain from point clouds: a minimum "elevation" surface map was created by searching for the lowest *ρ* values within a regular grid laid onto the (θ,*h*)-plane using a resolution of 1 rad × 1 m, respectively, to find stem surface. The obtained point class labeling (i.e. "stem points" or "branch points") was applied to the original T1 and T2 point clouds represented by the Cartesian coordinates for the next processing steps (Fig. 2D).

Finally, we reviewed the locations of the segmented trees to obtain reference information on which point cloud characterization at T1 represented the same tree individual characterized from the T2 point clouds. The point cloud reconstructions were also visually reviewed, and trees with incomplete point cloud reconstruction (i.e. only reconstructed from one side, while the opposite side of the tree remained occluded) were omitted from further analysis, resulting in 65 Scots pine trees.

Characterizing the identifying features of trees

Stem profile

The stem profile was estimated at T1 and T2 based on the obtained stem points using the methodology presented in Yrttimaa et al. (2019) and Yrttimaa et al. (2023a). First, diameters were measured along the stem at 10 cm intervals based on a least-squares circle fitting into points projected onto the (X,Y)-plane. The relationship between the consecutive diameter-height observations was examined to identify and remove outliers resulting from inaccurate diameter measurements using a second-order polynomial curve fit with a random sample consensus algorithm (Yrttimaa et al. 2023a). Based on this filtering, the height of the highest successful diameter observation was marked as the height up to which the stem could be reliably reconstructed by the point clouds. All points above this stem reconstruction top height were considered to originate from branches and foliage (i.e. "branch points"), and thus, their point class labeling was updated accordingly. A cubic spline smoothing was then applied to estimate the stem taper curve, aiming to reduce unevenness in consecutive diameter observations and interpolate the missing diameters toward the top of the tree, considered as the maximum height of the individual tree point cloud (Yrttimaa et al. 2019).

Branching arrangement

Branch origins on the stem were located by identifying intersections between stem points and branch points at T1 and T2 (Yrttimaa et al. 2023a). It was assumed from tree morphology that branches connect structurally to the surface of the stem. These intersections were determined by a minimum 3D Euclidean

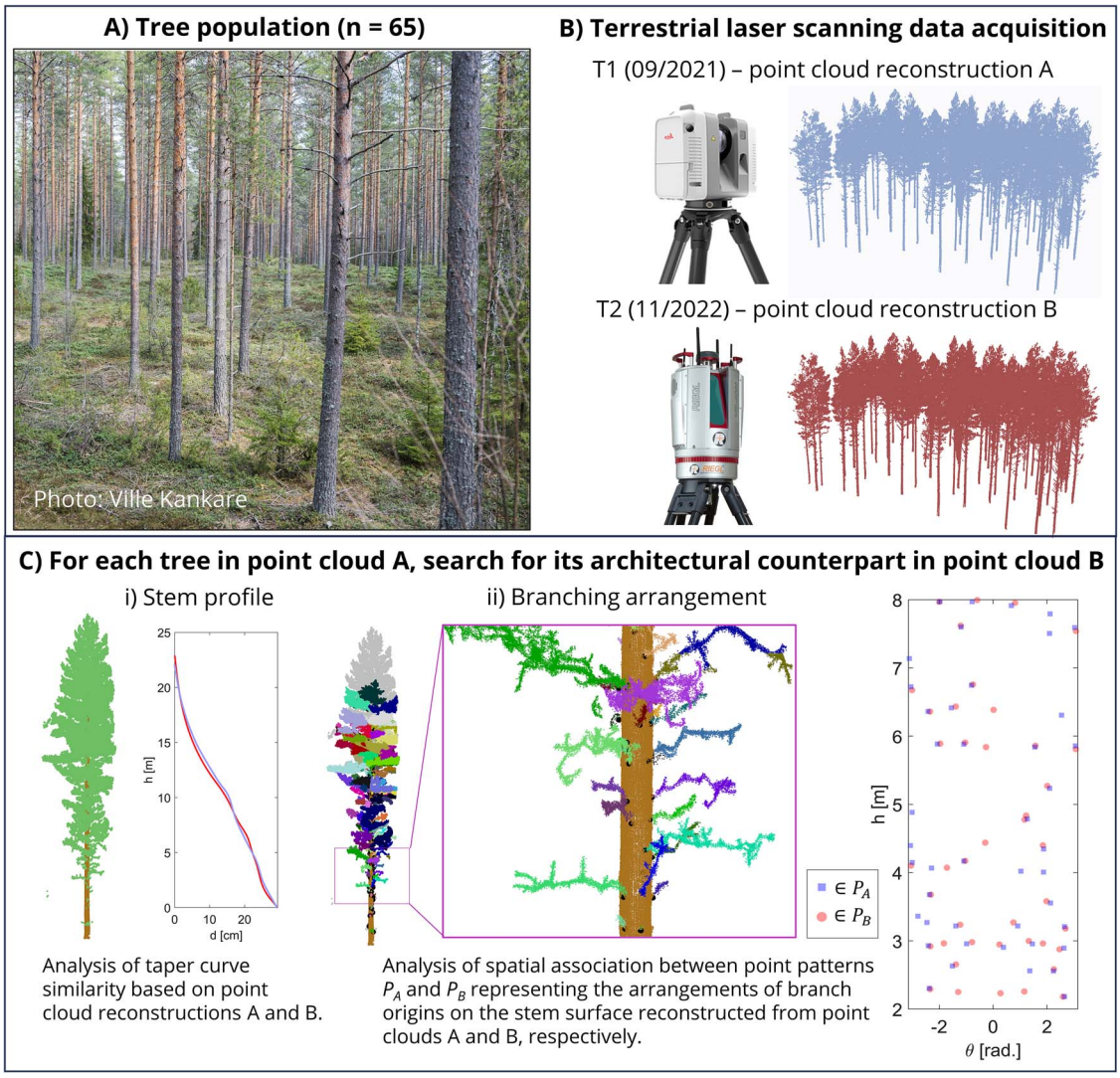

Figure 3. Experimental setup and methodology for investigating tree architectural uniqueness. Bitemporal terrestrial laser scanning was used to obtain point cloud reconstructions of a tree population (A, B). The assumption was that unique tree architectures allow individual identification based on stem profiles (diameters along the stem) and branching arrangements [branch origin patterns relative to height (h) and azimuth angle (θ)] (C).

distance (<1 cm) between stem points and branch points. Preliminary branch origins were extracted by connected component analysis, searching for stem and branch points within a 3D Euclidean distance $\pm\rho$ around the intersections. Further segmentation into clusters, with a maximum distance r between them, identified individual branch origins. Parameters ρ and r were set at 5 cm based on prior knowledge of the branching structure of Scots pine. Point cloud clusters representing individual branches were further labeled based on their connectivity with the obtained locations of the branch origins (Yrttimaa et al. 2023a). The locations of the branch origins were converted from Cartesian to cylinder representation, using information on stem orientation as previously described. This allowed the arrangement of branches along the stem surface to be presented as a pattern of points in 2D space defined by θ and h (Fig. 3).

Quantifying structural uniqueness of trees

Analyzing the capacity of terrestrial laser scanning to characterize the unique architecture of trees

To empirically test whether tree individuals feature a unique architecture, we investigated how accurately the tree individuals at one time point (T1) could be recognized among those characterized at a subsequent time (T2) based on the tree architecture. Successfully identifying the same individuals from two independent characterizations would confirm that they feature a unique architecture that can be quantified using point clouds. Identifiable features of an individual must be measurable and consistent over time for accurate recognition (e.g. Rai et al. 2020). To evaluate the reliability of these features, we first assessed how consistently tree architecture could be captured across two different sets of point cloud data.

We explored how well the stem profile and branching arrangement derived at T1 correspond to the respective characteristics derived at T2 for each individual tree. Correspondence in the stem profiles was analyzed by computing the root mean square error (RMSE) of stem diameters measured at 10 cm intervals, as well as the proportion of T2 diameter measurements that deviated <1.0 cm from the corresponding T1 measurement. This threshold was considered the measurement tolerance, accounting for both the measurement accuracy (Yrttimaa et al. 2020) and a 1-year stem diameter increment of some millimeters (Yrttimaa et al. 2023b). Correspondence in the branching arrangements was analyzed by computing how large a part of the branch origins identified from the T1 point cloud reconstruction could also be

identified from the T2 point cloud reconstruction. The two point patterns, representing the branching arrangements derived at T1 and T2, were compared, and the nearest neighbor points in T2 were searched for each point in T1. First, rotational alignment between the T1 and T2 point clouds was confirmed by manually identifying corresponding branch origins for four randomly sampled trees around the sample plot and computing $\Delta\theta$ that averaged to zero at the tree level. If this were not the case, the required θ translation between the T1 and T2 branch origin point patterns could have been determined using, for example, the iterative closest point (ICP) algorithm (Besl and McKay, 1992) combined with Delaunay triangulation–based triangulated irregular networks (TINs) to analyze geometric relationships between points and identify correspondences (McCullagh and Ross, 1980).

Then, nearest neighbor distances were computed on the stem surface by first obtaining $\Delta\theta$ and Δh and then converting $\Delta\theta$ from an angular distance (radians) to surface distance (meters) based on information of stem diameter at the given height. Point pairs separated by a maximum distance of 3 cm on the stem surface were considered as a "match," determined based on experiences gained from a previous study (Yrttimaa et al. 2023a). The number of these matching point pairs between the T1 and T2 characterizations was divided by the number of branch origins identified in T1 to estimate branching arrangement correspondence.

Considering the feasibility of TLS to characterize the lower part of the tree architecture rather than the upper crown structures, we delineated the analysis of the correspondence in stem profile and branching arrangement for the lower half of the tree height. We also analyzed the correspondence in different height intervals between 1 and 10 m above the ground to provide insights into the capacity of bitemporal TLS to characterize trees' unique architecture.

Identifying tree individuals based on their unique architecture

After investigating the capacity of TLS to characterize the potential identifying features of trees using bitemporal point clouds, we investigated whether the tree individuals can be separated from one another based on their unique architecture. To do so, we assumed that the T1 point cloud characterizations of each of the 65 Scots pine trees constitute a digitally reconstructed tree population A, while the T2 point cloud characterizations constitute a digitally reconstructed tree population B. It should be noted that these digitally reconstructed populations represent the same tree individuals with reconstructions based on two independent point cloud characterizations (see Fig. 3A and B). For each digitally reconstructed individual in population A, we searched for its architectural counterpart in population B, aiming at identifying the same tree individual from two different point cloud reconstructions (Fig. 3C). We tested two different approaches for the counterpart search: (i) based on similarity in stem profile and branching arrangement and (ii) based on similarity in branching arrangement only. With this test, we aimed to determine whether tree structural uniqueness can be quantified only by the branching arrangement and assess the contribution of the stem profile to the architectural uniqueness.

In the first approach, we shortlisted candidate individuals from population B based on similarity in stem profile by accepting a mean absolute difference of 1.0 cm in 70% of diameters along the stem within the 2–8 m height interval. The similarity in branching arrangement was then investigated among trees that featured a similar stem profile. In the second approach, the initial shortlisting based on stem profile was not conducted, and thus, similarity in branching arrangement with the subject tree in population A was investigated against all the trees in population B.

The similarity in branching arrangement was investigated using two different approaches based on the analysis of (i) spatial association and (ii) nearest neighbor distances between the obtained point patterns P_A and P_B representing the locations of branch origins along the stem for the subject tree from population A and its counterpart-candidate from population B, respectively. It was expected that there should be (i) a higher spatial association between P_A and P_B and (ii) a lower mean distance between nearest neighbors in P_A and P_B when P_A and P_B represent the branching arrangement of the same tree individual, compared to an alternative scenario where P_A and P_B represent the branching arrangement of different individuals (Fig. 4).

For the first approach, we applied the Spatial Pattern Analysis using the Closest Events (SPACE) approach (Soltisz et al. 2023). The procedure included analyzing the spatial relationship of P_A relative to P_B ($P_A \rightarrow P_B$) based on spatial statistics on nearest neighbors. The 2D point patterns were converted to binary raster images at a resolution of 0.02 rad in θ and 2 cm in h. Nearest neighbor distances between P_A and P_B were computed to obtain a cumulative distribution function (CDF), showing the cumulative proportion of increasing nearest neighbor distances (see Fig. 4). The obtained CDF was compared with another CDF characterizing the cumulative proportion of nearest neighbor distances between P_A and each image element. Subtraction between the CDFs resulted in a ΔCDF, indicating the magnitude by which the obtained spatial relationship between P_A and P_B deviated from a random spatial relationship. The spatial association between P_A and P_B was then summarized as a spatial association index (SAI), indicating the maximum absolute difference between PDF and CDF. SAI reached values between [−1,1], with a negative value indicating spatial dispersion, a positive value indicating spatial aggregation, and a value around zero indicating a random spatial relationship. Finally, the counterpart candidate from population B, which eventually featured the highest spatial association in the branching arrangement, was then considered a correspondent reconstruction for the subject tree in population A, concluding the identification of the respective tree individual.

In the second approach, the similarity in branching arrangement was quantified as the mean distance between nearest neighbors in P_A and P_B. The counterpart candidate from population B that featured the lowest mean nearest neighbor distance in branch origins was then considered a correspondent reconstruction for the subject tree in population A, concluding the identification of the respective tree individual.

Accuracy assessment

Once the corresponding point cloud reconstruction from population B had been linked to each of the individuals represented by population A, the identification accuracy was assessed with reference information of which point cloud characterization at T1 represented the same tree individual characterized from the T2 point clouds. The identification accuracy was separately assessed by the employed approaches to determine whether the stem profile contributes to structural uniqueness or can it be solely determined by the branching arrangement.

Given the expectation that not all branch origins would be visible in the point clouds, we focused our analysis on those branch origins that were closely positioned on the stem surface. Thus, in addition to using all the observed branch origins for branching arrangement similarity analysis, we examined the feasibility of using a limited number of branch origins featuring

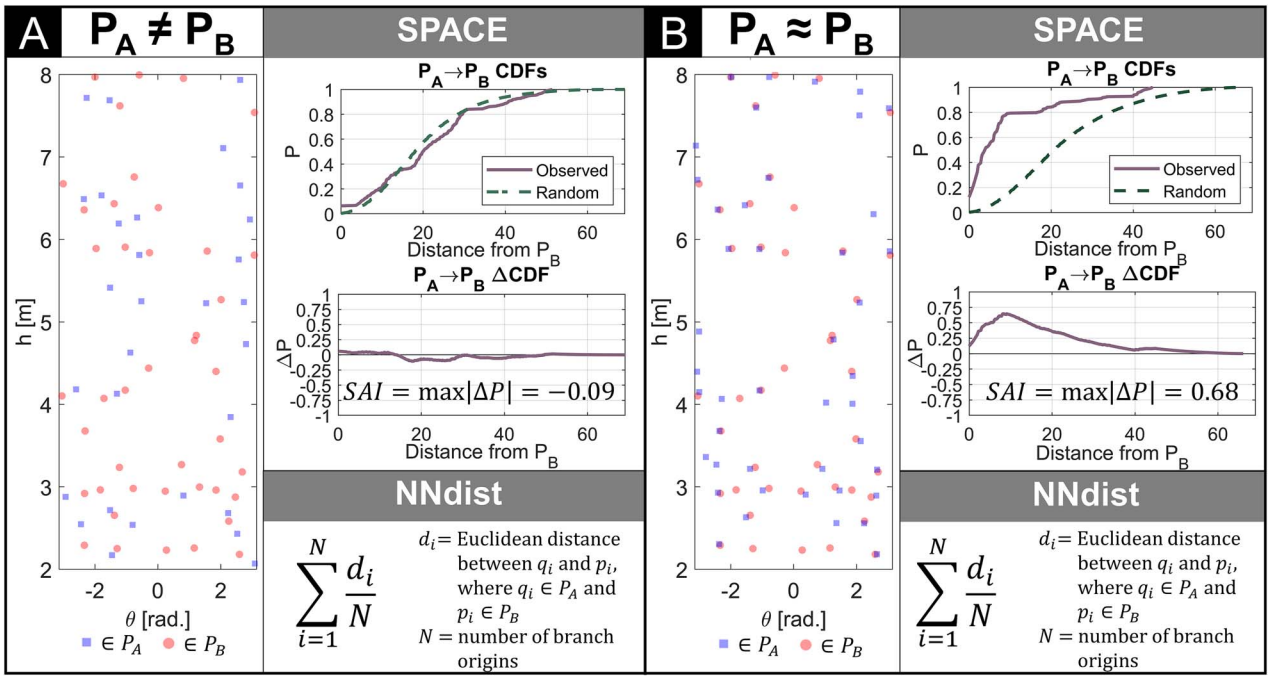

Figure 4. The similarity of branching arrangements was analyzed by comparing the spatial association between point patterns P_A and P_B, representing branch origin locations derived from independent point cloud reconstructions A and B, respectively. Two methods were used: (1) Spatial Pattern Analysis using Closest Events (SPACE) and (2) mean distance to N nearest neighbor points (NNdist). In the SPACE method, a spatial association index (SAI) was computed as the maximum absolute deviation between the observed and random cumulative distribution functions (CDFs). For NNdist, the mean distance between N nearest neighbor branch origin pairs was computed. P_B patterns with the highest SAI or lowest NNdist were considered counterparts to P_A. (A) shows nonmatching patterns (different individuals), and (B) shows matching patterns (same individual).

N lowest nearest neighbor distances between P_A and P_B, with N ranging from 5 to 30 with steps of 5. We also analyzed how the identification accuracy was affected when the identifying features were obtained from different height intervals between 1 and 10 m above the ground. To assess minimum requirements for tree identification, we analyzed the contribution of stem profile similarity assessment for identification as well as the minimum number of branch origin pairs to be identified from P_A and P_B that still resulted in the correct identification of individuals.

Results

Capacity of terrestrial laser scanning to characterize the unique architecture of trees

The experiments on a stem section between 1 and 10 m in height showed that 87.7% of diameter observations along the stem at T2 deviated <1.0 cm and 94.9% <1.5 cm from the respective T1 measurements. Depending on the stem section investigated, RMSE in the diameter observations ranged between 0.4 and 0.7 cm. Agreement between T1 and T2 in stem profile characterization increased for shorter stem sections positioned lower on the stem (Fig. 5A and B).

The number of branch origins observed from the T1 point cloud reconstruction ranged between 16 and 114 (mean 57) for the stem section between 1 and 10 m in height. From this stem section, an average of 10 branch origins (range 0–38, standard deviation 9.2) were identified also from the T2 point cloud reconstruction at a positional accuracy of <3 cm and 19 branches (range 1–64, standard deviation 14.5) at an accuracy of <5 cm. The number of branch origins observed at T1 and also identified at T2 decreased when the stem section got shorter or was positioned lower on the stem (Fig. 5C–E). The higher the stem section reached, the lower the mean distance between the five nearest neighbor branch origins (Fig. 5F).

Identifying tree individuals based on their unique architecture

Out of the 65 trees studied, 52 trees (80.0%) were identified from the independent point cloud characterizations based on their architecture. The highest identification accuracy was obtained when stem profile shortlisting was applied prior to the analysis of branching arrangement similarity that relied on the mean distance to the 10 nearest neighbor branch origins (NNdist) between P_A and P_B. The accuracy was only slightly influenced by the number of branch origins used, with a minimum value of 72.3%). The best results were obtained when 10–20 branches were considered, while using fewer or more branches slightly reduced the accuracy (Fig. 6). When the branching arrangement similarity analysis was based on the SPACE approach, the identification accuracy increased along with the number of nearest neighbor branches identified from the point cloud reconstructions (Fig. 6). When all the observed branches were used, the identification accuracy was similar between the two methods.

Stem profile shortlisting prior to the branching arrangement similarity analysis enhanced the identification accuracy by up to 10.8%–15.4%-points depending on the applied method and the number of nearest neighbor branches utilized in the identification (Fig. 6). Computed as the relative enhancement in tree identification accuracy, the contribution of stem profile in tree identification varied between 2.0% and 14.6% while branching arrangement accounted for an 85.4%–98.0% contribution.

Assessment of the minimum requirements for tree identification

After finding the best-performing approach for tree identification at a fixed stem height interval, we analyzed how the tree identification performance was influenced by the length and vertical position of the stem section under investigation. The results showed that the unique architecture enabling tree identification

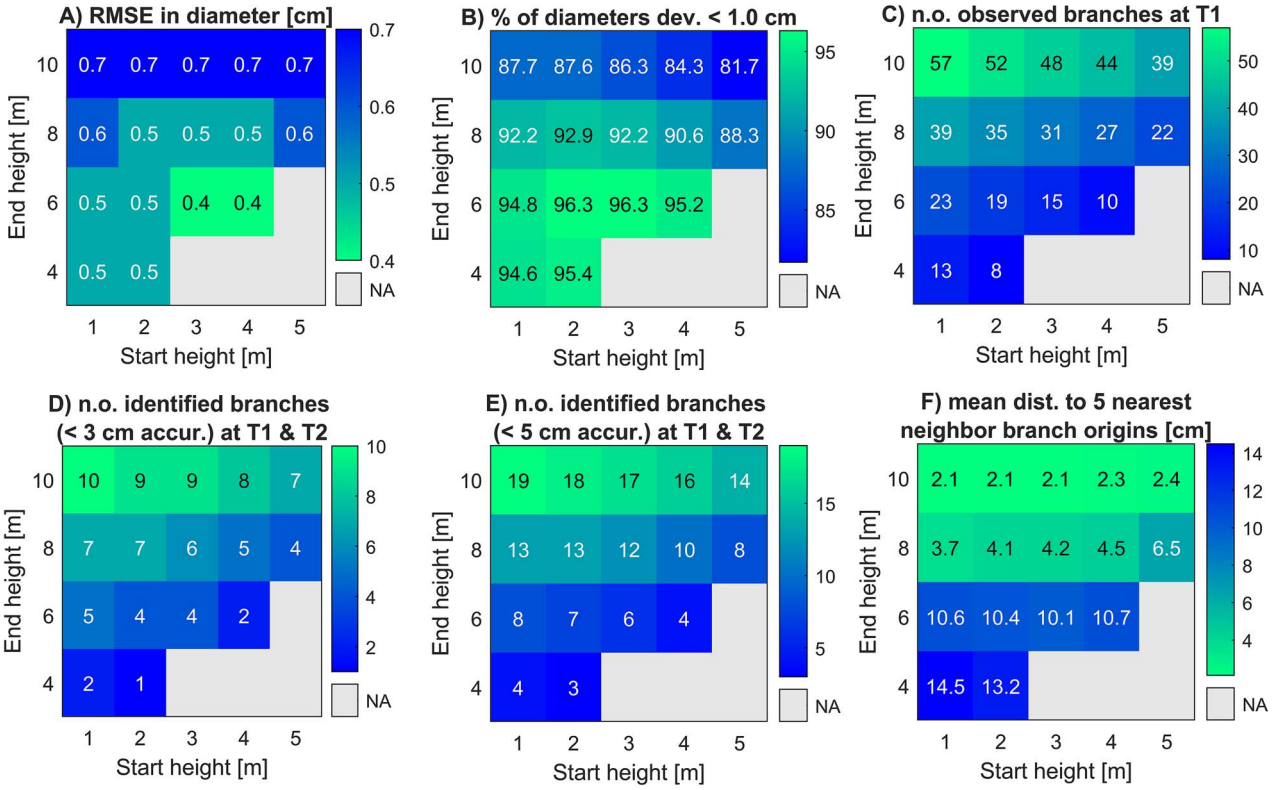

Figure 5. Assessment of bitemporal terrestrial laser scanning capacity to characterize stem profile and branching arrangement across different stem height intervals. (A) Mean root mean square error (RMSE) in diameter measurements along the stem. (B) Percentage of repeated diameter measurements deviating <1.5 cm. (C) Mean number of branch origins observed from the T1 (September 2021) point cloud reconstruction. (D) Mean number of branch origins identified in both T1 and T2 (November 2022) point cloud reconstructions at <3 cm positioning accuracy, and (E) at <5 cm positioning accuracy. (F) Mean distance measured between the five nearest neighbor branch origins from T1 and T2 reconstructions. NA = not analyzed.

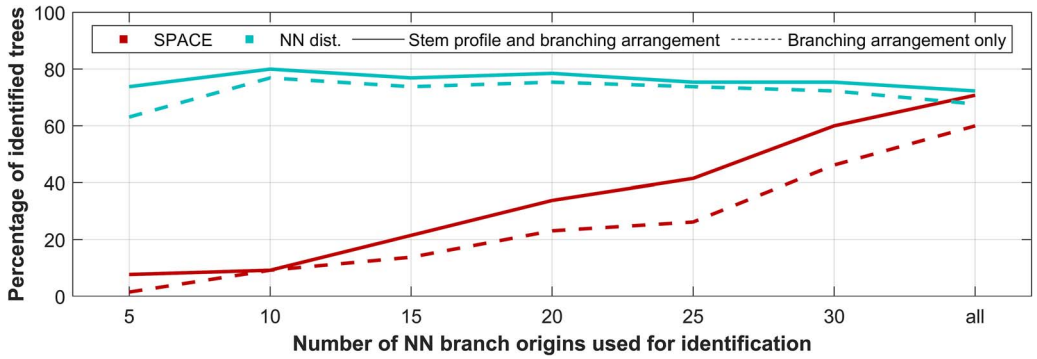

Figure 6. The percentage of correctly identified trees based on: (1) similarity in both stem profile and branching arrangement (solid line), and (2) similarity in branching arrangement alone (dashed line). The similarity in branching arrangement was assessed using either (a) spatial pattern analysis using closest events (SPACE) or (b) nearest neighbor distance (NN dist.) analysis. The investigations focused on a fixed stem section between 2 and 8 m above the ground, with the number of nearest neighbor (NN) branch origins used for identification varying as indicated along the *X*-axis.

was obtained for a larger proportion of Scots pine trees when the investigated stem section started below the height of 3 m and extended up to the height of 8 m (Fig. 7).

Assessment of the minimum requirements for tree identification revealed that 96.9% of such trees for which ≥5 branch origin pairs from P_A and P_B were identified with a 3 cm positioning accuracy ($n = 32$ out of 65 trees) could be identified from the point cloud reconstructions. The identification accuracy increased to 100% among trees for which ≥10 branch origin pairs were identified ($n = 20$).

The branching arrangement seemed to be the most determinant identifying feature, as none of the trees were identified solely based on stem profile similarity. However, shortlisting the candidates prior to the branching similarity analysis enhanced tree identification accuracy by 0%–7.7% when the identification was based on the mean distance among 10 nearest neighbor branch origins (Fig. 7). The enhancement was more prominent when the investigated stem section was shorter and was positioned lower on the stem, i.e. when the number of identified branches within the investigated stem section got smaller.

Assessment of the architectural properties between unidentified and identified trees showed that, while identified trees featured a larger number of branches observed at T1, their probability of being identified seemingly increased with an increasing

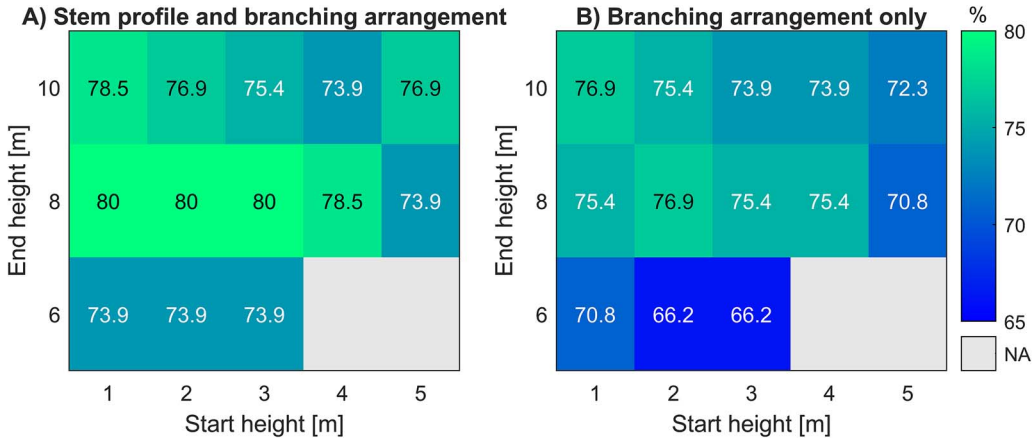

Figure 7. The percentage of correctly identified trees from the sampled population (n = 65) based on the assessment of: (A) similarity in both stem profile and branching arrangement and (B) similarity in branching arrangement alone, evaluated across different stem sections. Columns indicate the starting height of each stem section, while rows represent the length of the section extending upward from the starting height. The similarity in branching arrangement was determined using the nearest neighbor distance (NN dist.) analysis of 10 nearest branch origins. NA = not analyzed.

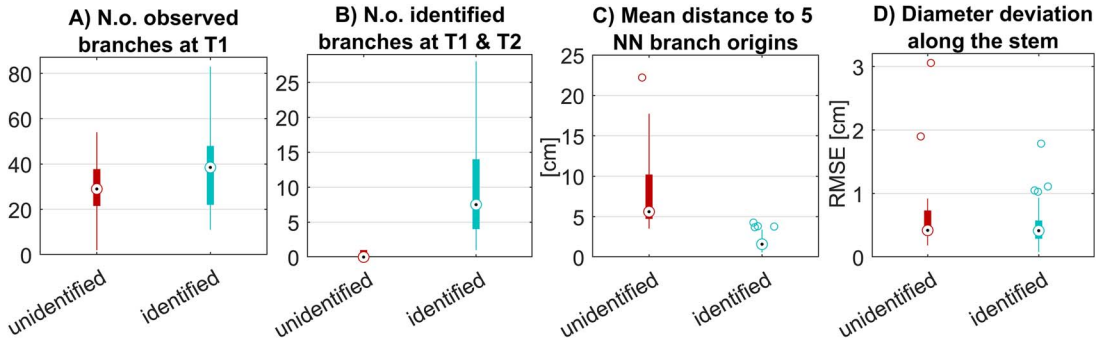

Figure 8. Comparison of the characteristics between trees identified and those not identified based on their architecture, as reconstructed from point clouds at T1 and T2. In each boxplot, the box represents the interquartile range (IQR), the middle point represents the median, the whiskers show the statistical range (i.e. 1.5 * IQR, equivalent to 99.3% confidence interval for normally distributed data), and the scattered circles represent outliers. NN = nearest neighbor, RMSE = root mean square error.

number of such branch origins that could be identified at both time points (Fig. 8). The identified trees also featured a lower mean distance to the five nearest neighbor branch origins when comparing P_A and P_B, while the stem profile characterization accuracy was rather similar between unidentified and identified trees.

Discussion

In this research, we investigated the capacity of TLS to capture the branching patterns of Scots pine trees with sufficient precision to distinguish individual trees, thereby empirically demonstrating their architectural uniqueness. We propose that through digital tree reconstruction, it is possible to identify tree individuals from bitemporal TLS data by examining the point cloud data of their structure, particularly the distribution of branches along the stem. In this study, we focused on assessing the effectiveness of TLS in depicting the unique architecture of trees, with findings showing a strong consistency in the characterizations of stem profiles at the lower part of the stem. Identifying exactly the same branch origins from two point cloud reconstructions proved to be more challenging, yet up to 10 matching branch origins were identified on average when considering <3 cm positional accuracy on a stem section between 1 and 10 m height. Subsequent experiments showed that the level of detail achieved in characterizing tree architecture was sufficient for identifying individual trees. We found that trees could be reliably identified if 10 or more pairs of branch origins were discerned from independent point cloud reconstructions. This suggests that tree architecture can serve as a unique distinguishing feature, offering opportunities for various applications that necessitate tree identification based on characteristics other than geospatial location.

Tree architectural uniqueness was presumed based on current knowledge of how tree architecture is a realization of the growth process driven by various external drivers with effects varying by individuals and growing environments (Valladares and Niinemets, 2007). However, it has remained unknown to what extent the architectural details should be quantified to distinguish two individuals from each other. It was already known that close-range sensing techniques such as TLS enable millimeter-level detail in observations of tree architecture (Hackenberg et al. 2014), providing the means for measuring stem profiles (Simonse et al. 2003; Liang et al. 2013) and identifying individual branches (Demol et al. 2022; Yrttimaa et al. 2023a), for example. Nevertheless, even state-of-the-art technology cannot capture all the architectural details due to the complex structure of trees and their surrounding environment (Côté et al. 2011; Liang et al. 2016). It is important to note that TLS-based characterization of the structures of interest requires their digitization during data acquisition (i.e. remaining within the scanner's line of sight) and subsequent identification and quantification using computational point cloud processing methods (Yrttimaa 2021). Thus, the

current technical and methodological capacities in point cloud-based tree characterization define the limits for the extent to which the tree's architectural uniqueness can be assessed: an incomplete 3D reconstruction—one that omits some architectural details—should provide a sufficient basis for this assessment to serve practical applications.

The experiments revealed that an exact reconstruction of the entire tree architecture was unnecessary for determining the architectural uniqueness of trees within the studied tree population ($n = 65$). Within managed boreal forest conditions, characterizing the profile of the lower part of the stem at <1.5 cm accuracy, as well as distinguishing a small number (≥10) of branch origins on the surface of the respective stem section, seemed sufficient to determine unique tree architecture and enable the identification of tree individuals without knowledge of their geospatial location. Comparison of tree identification accuracies between the applied methods highlighted the contributions of different architectural characteristics to tree uniqueness. The branching arrangement emerged as the most determinant identifying feature, followed by the stem profile, which contributed an average of 4% to the overall identifying accuracy. However, we note that our experimental setup employed a limited number of trees. Caution is, therefore, required when interpreting the universality of our findings. Regardless, we point to data and methods that demonstrate that the unique architecture of trees can be determined solely by a point pattern representing the locations of only ten branch origins on the stem surface. The findings also demonstrate the level and magnitude of individual tree-level detail required for quantifying the architectural uniqueness of trees. In this study, we only focused on branch locations, though incorporating additional factors such as branch base diameter could have served as weights when determining correspondences between point cloud reconstructions. Nevertheless, we recommend further investigations to assess the validity of the investigated hypothesis across different forest stands and tree species.

The process of identifying the same tree individual from two independent point cloud reconstructions aimed to demonstrate that each tree has unique structural traits that uniquely set it apart within a population. The arrangement of branches along the stem surface was desired as a nondestructively measurable characteristic that also captures the complexity of crown architecture in a simplified manner. The branching arrangement was presented as a pattern of points defined by θ and h, making the representation invariant over time for branches not breaking off. A comparison of these point patterns obtained from the same individual and also from different individuals revealed that, while single branch origins could spatially overlap by chance, it was very unlikely that other individuals would feature multiple overlapping branches. Thus, similarity in the branching arrangement was expected to identify tree individuals. We used two approaches to quantify this similarity, considering nearest neighbor distances between P_A and P_B. The SPACE approach enables an assessment of how much the observed distribution of nearest neighbor distances differs from a distribution of distances to a random point pattern, while NNdist measures the actual mean nearest neighbor distance to a selected number of nearest neighbor branch origins. The NNdist appeared to be the better performing of the two tested methods, being more intolerant to the number of branch origin pairs identified between the point cloud reconstructions. However, both approaches successfully identified the corresponding point cloud reconstructions representing the same tree individual when numerous branches were identified between the point cloud reconstructions. This underscores the robustness of the presented method for quantifying the architectural uniqueness of trees through branching arrangement characterization. The key lies in reconstructing the tree's branching structure with sufficient accuracy to identify the origins of a handful of branches. Once this is achieved, alternative methods can be applied to quantify the similarity between the resulting point patterns and identify correspondences.

While the branching arrangement seemed to be the most determinant identifying feature, the presented approach for quantifying the architectural uniqueness of trees ultimately relied on the capacity and accuracy of the point cloud–based methods for identifying individual branches and their origins on the stem surface. The method applied in this study was initially presented in Yrttimaa et al. (2023a), where its branch identification performance was validated using the same TLS data acquisition that corresponds to the T2 TLS in this study. The trees used for validation ($n = 100$) were randomly sampled across the sample plot and did not entirely represent the same population investigated in this study. Furthermore, the methodology was not specifically tailored to the data used here but was developed for characterizing the branching structure of similar types of trees. The trees selected for method development and validation in Yrttimaa et al. (2023a) were Scots pines typical of boreal forests, featuring a bole-like main stem, relatively small-diameter branches, and a sparse lower crown structure (see Fig. 1). These characteristics enabled detailed reconstruction of the first half of the stem and respective branches. Experiments carried out in Yrttimaa et al. (2023a) showed that branches located at 10%–50% relative height and visible in the point cloud were automatically identified at an accuracy of 0.91 with a recall of 0.85 and a precision of 0.97. These figures indicate that it is likely that the observed branch origins actually represented the origins of branches, while a considerable proportion of branches could still have remained unidentified.

Although the accuracy of identifying branches was not separately validated for the population investigated in this study, a similar level of accuracy could be expected for the identification of branch origins at T1 and T2 located at the 1–10 m height interval. However, we note that the observations were repeated in time using point clouds acquired with slightly different scan setups, resulting in different point cloud reconstructions. In this case, no rotational misalignment was detected between the T1 and T2 point clouds. However, if such misalignment had occurred, an iterative procedure to determine the corresponding rotational shift ($\Delta\theta$) required for data alignment would have been necessary. If the T2 branching arrangements were derived independently from each tree, for example after harvesting, rotational reorientation would need to be applied to each candidate before comparing P_A and P_B to identify correspondences. Although this was not investigated here, methodologies such as Delaunay triangulation–based TINs (McCullagh and Ross 1980) could be employed to identify geometric similarities, enabling the application of algorithms such as ICP (Besl and McKay 1992) to compute the required coordinate transformations automatically.

Regardless, both T1 and T2 point clouds were still processed independently, including height normalization and tree characterization procedures. The branch origins were determined based on the intersections between the stem surface and branches, meaning that the obtained location can vary depending on branch diameter and the direction from which the stem–branch intersection became scanned. Thus, it is more than possible that the observed positions of branch origins on the stem surface deviated by several centimeters. In this respect, the applied 3 cm accuracy in distinguishing branch origin pairs between the point

cloud reconstructions can be considered rather conservative, and decreasing the accuracy to 5 or even 7 cm could be justified as well. While the 3 cm accuracy threshold resulted in an average agreement of 17.3% between the observed branching arrangements, the 5 and 7 cm thresholds showed average agreements of 33.8% and 47.1%, respectively.

While methodological improvements in the applied point cloud processing algorithms may enhance the characterization of branching arrangement and thus the quantification of architectural uniqueness, the properties of the point clouds used still have the most significant contribution in how well individual branches become identified. In this study, we used TLS that represents the state-of-the-art geometric accuracy in the acquired point clouds. However, the applied scan setup was planned to capture the characteristics of an entire 0.4 ha forest stand. Focusing on capturing the complete architecture of individual trees instead would have required a more intensive scan setup to ensure that each individual becomes scanned from all perspectives. However, in this experimental setup, we aimed to use point cloud data that would realistically represent the type of 3D reconstructions that could be available for operational use. In such cases, it is assumed that the utilized point clouds may vary in acquisition method and characteristics, with the most recent acquisition likely being the most precise and complete due to advancements in sensor technology. It is also important to note that if the presented methodology for quantifying tree architectural uniqueness is used more widely, the utilized point clouds are most likely acquired cost-effectively from a mobile platform during a forest operation. Compared to TLS, mobile laser scanning (MLS), conducted using a hand-held, backpack-mounted, or vehicle-mounted laser scanner (Hunčaga et al. 2020), tends to provide an enhanced point cloud coverage per allocated resources, but—at least currently—with the cost of decreased geometric accuracy in the obtained point clouds (Balenović et al. 2021). Even with current technology, a stem profile and information about the branching arrangement can be reconstructed from MLS point clouds as well (e.g. Hyyppä et al. 2020, Winberg et al. 2023). The results of this study suggest that the key identifying features of trees, notably a select number of branch origins, might also be derived from point clouds obtained via mobile platforms instead of stationary ones.

The experiments conducted herein indicate that the distinctive architecture of Scots pine trees can be captured and quantified using point cloud data of stem profiles and branching patterns. Through our experimental setup and methodology, we provided empirical evidence that tree individuals feature a unique, measurable architecture and that the architectural uniqueness could be used for applications requiring the identification of tree individuals. While validating the proposed hypothesis, we introduced an approach to identifying tree individuals based on two independent point cloud reconstructions. This approach can also be implemented in an identification task that could benefit, e.g. tracking the origin of trees during wood procurement. The findings of this study suggest that if we have reconstructed the architecture of trees the first time when standing in the forest and then the second time during a harvesting operation, we could identify which trees have been harvested and used as raw material for certain wood products. Another option is to automatically reconstruct the branching pattern when the timber arrives at the factory by identifying knots and their positions in the wood using X-ray computer tomography (CT) (e.g. Longuetaud et al. 2012). By comparing laser scanning–derived and CT-derived branching patterns, it may then be possible to establish a link between harvested trees and their respective timber products. Currently, such tracking is organized through artificial marking (e.g. radio-frequency identification tags, paint labels; Müller et al. 2019), while photographing the cross-sections of the harvested logs has been shown as a feasible alternative that may be automated (e.g. Schraml et al. 2016, Holmström et al. 2023). An additional possible area of application is to use tree-identifying features in, e.g. growth and yield purposes where it is essential to confirm that analyses of structural changes are targeted to the same tree individuals (Weiskittel et al. 2011). Tree identity information could also be used for solving geolocalization problems related to simultaneous localization and mapping and the acquisition and georeferencing of multisensorial point clouds from mobile platforms within under canopy conditions where the limited signal from GNSSs does not provide sufficient positioning accuracy (e.g. Tang et al. 2015, Muhojoki et al. 2024, Zhou et al. 2024).

Conclusion

The experiments in this study showed that individual Scots pine trees can be characterized using close-range laser scanning with a level of geometric accuracy that allows for tree identification based on architectural features. The positioning of branch origins along the stem was identified as a key distinguishing characteristic, essentially serving as a tree's "fingerprint." While the small sample size suggests that the findings should be interpreted with caution, our methodology demonstrated that the complex intricate structure of a tree's branching can be simplified and quantified as a pattern of 2D points. This simplification allows for effective comparisons of branching patterns across different point cloud reconstructions. Individual trees can be accurately identified by evaluating the similarity of these 2D point patterns, particularly using methods based on nearest-neighbor distances. However, more extensive experiments across different forest types are needed to provide more generalizable findings.

Identifying individual branches is crucial for establishing the architectural uniqueness of trees, suggesting a need for high-quality point cloud data collection that accurately characterizes each tree. Terrestrial point clouds are particularly effective for examining the lower stem section, where branches join the stem and are visible to the sensor. Complete reconstruction of the tree's architecture does not appear necessary, but the analyzed stem section should include a sufficient count of branches—evidently at least 10 for Scots pine trees in managed boreal forests as per our findings. The stem profile's role in determining a tree's unique architecture appears minimal. However, initially narrowing down potential matches based on stem profile before conducting detailed comparisons of branching patterns is crucial for accurately identifying individual trees within a large population.

Taken in combination, the experiments implemented offer empirical evidence for the structural uniqueness of trees located in a managed forest stand with uniform growing conditions throughout. This underscores the effectiveness of close-range laser scanning for detailing the distinct architectural features of trees and suggests the potential of utilizing tree architecture as a means of identification. The methodology introduced here can benefit applications requiring tree origin tracing, such as tracking wood to its source.

Acknowledgements

This work would not have been possible without the Measuring Spatiotemporal Changes in Forest Ecosystem Research Infrastructure (www.scanforest.fi).

Author contributions

Tuomas Yrttimaa (Conceptualization, Formal analysis, Investigation, Methodology, Software, Writing—original draft), Samuli Junttila (Investigation, Writing—review & editing), Juha Hyyppä (Funding acquisition, Resources), Markus Holopainen (Funding acquisition, Resources), Michael A. Wulder (Writing—review & editing), and Mikko Vastaranta (Conceptualization, Funding acquisition, Resources, Writing—review & editing).

Conflict of interest statement: None declared.

Funding

This study was supported by the Research Council of Finland through funding provided for the UNITE flagship [grant numbers 337127, 357906]; Diversity4Forests project [grant numbers 348643, 348644]; and Quality4Trees [grant numbers 334001, 334002]. It should be noted that the funding for the Diversity4Forests project originates from the European Union's NextGenerationEU initiative. S.J. was also funded by the European Union (ERC-2023-STG) [grant number 101116404]. Views and opinions expressed are, however, those of the authors only and do not necessarily reflect those of the European Union or the European Research Council Executive Agency. Neither the European Union nor the granting authority can be held responsible for them.

Data availability

The data underlying this article are available on the website of the Scanforest research infrastructure at www.scanforest.fi/data.

References

Åkerblom M, Raumonen P, Mäkipää R. *et al.* Automatic tree species recognition with quantitative structure models *Remote Sens Environ*. 2017;**191**:1–12. https://doi.org/10.1016/j.rse.2016.12.002.

Balenović I, Liang X, Jurjević L. *et al.* Hand-held personal laser scanning–current status and perspectives for forest inventory application *Cro J For Eng*. 2021;**42**:165–83. https://doi.org/10.1016/j.rse.2016.12.002.

Béland M, Widlowski JL, Fournier RA. *et al.* Estimating leaf area distribution in savanna trees from terrestrial LiDAR measurements *Agric For Meteorol*. 2011;**151**:1252–66. https://doi.org/10.1016/j.agrformet.2011.05.004.

Besl PJ, McKay ND. Method for registration of 3-D shapes *In Sensor fusion IV: control paradigms and data structures*. 1992;**1611**:586–606.

Bogdanovich E, Perez-Priego O, El-Madany TS. *et al.* Using terrestrial laser scanning for characterizing tree structural parameters and their changes under different management in a Mediterranean open woodland *For Ecol Manage*. 2021;**486**:118945, 118945, https://doi.org/10.1016/j.foreco.2021.118945.

Brousseau L, Bonal D, Cigna J. *et al.* Highly local environmental variability promotes intrapopulation divergence of quantitative traits: An example from tropical rain forest trees *Ann Bot*. 2013;**112**:1169–79. https://doi.org/10.1093/aob/mct176.

Calders K, Adams J, Armston J., Bartholomeus H, Bauwens S, Bentley LP, Chave J, Danson FM, Demol M, Disney M, Gaulton R, Krishna Moorthy SM, Levick SR, Saarinen N, Schaaf C, Stovall A, Terryn L, Wilkes P, Verbeeck H Terrestrial laser scanning in forest ecology: Expanding the horizon *Remote Sens Environ*. 2020;**251**:112102, 112102. https://doi.org/10.1016/j.rse.2020.112102.

Callaway RM, Pennings SC, Richards CL. Phenotypic plasticity and interactions among plants *Ecology*. 2003;**84**:1115–28. https://doi.org/10.1890/0012-9658(2003)084[1115:PPAIAP]2.0.CO;2.

Côté JF, Fournier RA, Egli R. An architectural model of trees to estimate forest structural attributes using terrestrial LiDAR *Environ Model Software*. 2011;**26**:761–77. https://doi.org/10.1016/j.envsoft.2010.12.008.

Demol M, Wilkes P, Raumonen P. *et al.* Volumetric overestimation of small branches in 3D reconstructions of Fraxinus excelsior *Silva Fenn*. 2022;**56**:10550. https://doi.org/10.14214/sf.10550.

Disney MI, Boni Vicari M, Burt A. *et al.* Weighing trees with lasers: Advances, challenges and opportunities *Interface Focus*. 2018;**8**:20170048. https://doi.org/10.1098/rsfs.2017.0048.

Enquist BJ, West GB, Brown JH. Extensions and evaluations of a general quantitative theory of forest structure and dynamics *PNAS*. 2009;**106**:7046–51. https://doi.org/10.1073/pnas.0812303106.

Gamfeldt L, Snäll T, Bagchi R. *et al.* Higher levels of multiple ecosystem services are found in forests with more tree species *Nat Commun*. 2013;**4**:1340. https://doi.org/10.1038/ncomms2328.

Gillet F. Plant competition. In: Jorgensen SE, Fath BD, (eds.). *Encyclopedia of Ecology*. Elsevier, 2008, 2783–93.

Hackenberg J, Morhart C, Sheppard J. *et al.* Highly accurate tree models derived from terrestrial laser scan data: A method description *Forests*. 2014;**5**:1069–105. https://doi.org/10.3390/f5051069.

Henning JG, Radtke PJ. Ground-based laser imaging for assessing three-dimensional forest canopy structure *Photogramm Eng Remote Sens*. 2006;**72**:1349–58. https://doi.org/10.14358/PERS.72.12.1349.

Holmström E, Raatevaara A, Pohjankukka J, Korpunen H, Uusitalo J. Tree log identification using convolutional neural networks *Smart Agric Technol*. 2023;**4**:100201, 100201. https://doi.org/10.1016/j.atech.2023.100201.

Hunčaga M, Chudá J, Tomaštík J. *et al.* The comparison of stem curve accuracy determined from point clouds acquired by different terrestrial remote sensing methods *Remote Sens (Basel)*. 2020;**12**:2739. https://doi.org/10.3390/rs12172739.

Hyyppä E, Kukko A, Kaijaluoto R. *et al.* Accurate derivation of stem curve and volume using backpack mobile laser scanning *ISPRS J Photogramm Remote Sens*. 2020;**161**:246–62. https://doi.org/10.1016/j.isprsjprs.2020.01.018.

Jain AK, Flynn P, Ross AA, (eds.). *Handbook of Biometrics*. Springer Science & Business Media, 2007.

Kobe RK, Coates KD. Models of sapling mortality as a function of growth to characterize interspecific variation in shade tolerance of eight tree species of northwestern British Columbia *Can J For Res*. 1997;**27**:227–36. https://doi.org/10.1139/x96-182.

Larson PR. *Wood Formation and the Concept of Wood Quality*. School of Forestry, Bulletin No: Yale University, 1969, 74.

Liang X, Kankare V, Hyyppä J. *et al.* Terrestrial laser scanning in forest inventories *ISPRS J Photogramm Remote Sens*. 2016;**115**:63–77.

Liang X, Kankare V, Yu X. *et al.* Automated stem curve measurement using terrestrial laser scanning *IEEE Trans Geosci Remote Sens*. 2013;**52**:1739–48.

Longuetaud F, Mothe F, Kerautret B. *et al.* Automatic knot detection and measurements from X-ray CT images of wood: A review and validation of an improved algorithm on softwood samples *Comput Electron Agric*. 2012;**85**:77–89. https://doi.org/10.1016/j.compag.2012.03.013.

Luoma V, Yrttimaa T, Kankare V. *et al.* Revealing changes in the stem form and volume allocation in diverse boreal forests using two-date terrestrial laser scanning *Forests*. 2021;**12**:835. https://doi.org/10.3390/f12070835.

Malhi Y, Jackson T, Patrick Bentley L. *et al.* New perspectives on the ecology of tree structure and tree communities through terrestrial laser scanning *Interface Focus*. 2018;**8**:20170052. https://doi.org/10.1098/rsfs.2017.0052.

McCullagh MJ, Ross CG. Delaunay triangulation of a random data set for isarithmic mapping *Cartogr J*. 1980;**17**:93–9. https://doi.org/10.1179/caj.1980.17.2.93.

Morsdorf F, Kükenbrink D, Schneider FD. *et al.* Close-range laser scanning in forests: Towards physically based semantics across scales *Interface Focus*. 2018;**8**:20170046. https://doi.org/10.1098/rsfs.2017.0046.

Muhojoki J, Hakala T, Kukko A. *et al.* Comparing positioning accuracy of mobile laser scanning systems under a forest canopy *Sci Remote Sens*. 2024;**9**:100121. https://doi.org/10.1016/j.srs.2024.100121.

Müller F, Jaeger D, Hanewinkel M. Digitization in wood supply–a review on how industry 4.0 will change the forest value chain *Comput Electron Agric*. 2019;**162**:206–18. https://doi.org/10.1016/j.compag.2019.04.002.

Oliver CD, Larson BC. *Forest Stand Dynamics*Updated edn. John Wiley and Sons, 1996.

Pan Y, Birdsey RA, Fang J. *et al.* A large and persistent carbon sink in the world's forests *Science*. 2011;**333**:988–93. https://doi.org/10.1126/science.1201609.

Pingel TJ, Clarke KC, McBride WA. An improved simple morphological filter for the terrain classification of airborne LIDAR data *ISPRS J Photogramm Remote Sens*. 2013;**77**:21–30. https://doi.org/10.1016/j.isprsjprs.2012.12.002.

Popescu SC, Wynne RH. Seeing the trees in the forest *Photogramm Eng Remote Sens*. 2004;**70**:589–604. https://doi.org/10.14358/PERS.70.5.589.

Pregitzer KS, Euskirchen ES. Carbon cycling and storage in world forests: Biome patterns related to forest age *Glob Chang Biol*. 2004;**10**:2052–77. https://doi.org/10.1111/j.1365-2486.2004.00866.x.

Rai V, Mehta K, Jatin J. *et al.* Automated biometric personal identification-techniques and applications. 4th international conference on intelligent computing and control systems (ICICCS) *Madurai, India*. 2020;**2020**:1023–30. https://doi.org/10.1016/j.isprsjprs.2012.12.002.

Reinhardt D, Kuhlemeier C. Plant architecture *EMBO Rep*. 2002;**3**:846–51. https://doi.org/10.1093/embo-reports/kvf177.

Ritter T, Nothdurft A. Automatic assessment of crown projection area on single trees and stand-level, based on three-dimensional point clouds derived from terrestrial laser-scanning *Forests*. 2018;**9**:237. https://doi.org/10.3390/f9050237.

Ritter T, Schwarz M, Tockner A. *et al.* Automatic mapping of forest stands based on three-dimensional point clouds derived from terrestrial laser-scanning *Forests*. 2017;**8**:265. https://doi.org/10.3390/f8080265.

Rosell JR, Llorens J, Sanz R. *et al.* Obtaining the three-dimensional structure of tree orchards from remote 2D terrestrial LIDAR scanning *Agric For Meteorol*. 2009;**149**:1505–15. https://doi.org/10.1016/j.agrformet.2009.04.008.

Schraml R, Hofbauer H, Petutschnigg A. *et al.* On rotational pre-alignment for tree log identification using methods inspired by fingerprint and iris recognition *Mach Vis Appl*. 2016;**27**:1289–98. https://doi.org/10.1007/s00138-016-0814-2.

Simonse M, Aschoff T, Spiecker H. *et al.* Automatic determination of forest inventory parameters using terrestrial laser scanning. In: Proceedings of the scandlaser scientific workshop on airborne laser scanning of forests 2003. Sveriges Lantbruksuniversitet *Umeå*. 2003;252–8.

Soltisz AM, Craigmile P, Veeraraghavan R. Spatial pattern analysis using closest events (SPACE): A nearest neighbor point pattern analysis framework for assessing spatial relationships from image data *Microsc Microanal*. 2023;**ozae022**.

Srinivasan S, Popescu SC, Eriksson M. *et al.* Multi-temporal terrestrial laser scanning for modeling tree biomass change *For Ecol Manage*. 2014;**318**:304–17. https://doi.org/10.1016/j.foreco.2014.01.038.

Taiz L, Zeiger E. *Plant Physiology*. 5th edition. Sunderland, MA: Sinauer Associates, 2010, 464.

Tang J, Chen Y, Kukko A. *et al.* SLAM-aided stem mapping for forest inventory with small-footprint mobile LiDAR *Forests*. 2015;**6**:4588–606. https://doi.org/10.3390/f6124390.

Valladares F, Niinemets U. The architecture of plant crowns: From design rules to light capture and performance. In: Pugnaire F, Valladares F, (eds.). *Functional Plant Ecology*. New York, NY: Taylor and Francis, 2007.

Van der Zande D, Stuckens J, Verstraeten WW. *et al.* 3D modeling of light interception in heterogeneous forest canopies using ground-based LiDAR data *Int J Appl Earth Obs Geoinf*. 2011;**13**:792–800. https://doi.org/10.1016/j.jag.2011.05.005.

Waring RH, Running SW. *Forest Ecosystems: Analysis at Multiple Scales*. Elsevier, 2010.

Weiskittel AR, Hann DW, Kershaw JA. *et al. Forest Growth and Yield Modeling*. John Wiley & Sons, 2011.

Winberg O, Pyörälä J, Yu X. *et al.* Branch information extraction from Norway spruce using handheld laser scanning point clouds in Nordic forests *ISPRS Open J Photogramm Remote Sens*. 2023;**9**:100040. https://doi.org/10.1016/j.ophoto.2023.100040.

Xi Z, Hopkinson C, Rood SB. *et al.* See the forest and the trees: Effective machine and deep learning algorithms for wood filtering and tree species classification from terrestrial laser scanning *ISPRS J Photogramm Remote Sens*. 2020;**168**:1–16. https://doi.org/10.1016/j.isprsjprs.2020.08.001.

Yrttimaa T. Characterizing tree communities in space and time using point clouds *Dissertationes Forestales*. 2021;**314**:52. https://doi.org/10.14214/df.314.

Yrttimaa T, Kankare V, Luoma V. *et al.* A method for identifying and segmenting branches of scots pine (Pinus sylvestris L.) trees using terrestrial laser scanning *Forestry*. 2023a;cpad062. https://doi.org/10.14214/df.314.

Yrttimaa T, Junttila S, Luoma V. *et al.* Capturing seasonal radial growth of boreal trees with terrestrial laser scanning *For Ecol Manage*. 2023b;**529**:120733. https://doi.org/10.1016/j.foreco.2022.120733.

Yrttimaa T, Saarinen N, Kankare V. *et al.* Performance of terrestrial laser scanning to characterize managed scots pine (Pinus sylvestris L.) stands is dependent on forest structural variation *ISPRS J Photogramm Remote Sens*. 2020;**168**:277–87. https://doi.org/10.1016/j.isprsjprs.2020.08.017.

Yrttimaa T, Saarinen N, Kankare V. *et al.* Investigating the feasibility of multi-scan terrestrial laser scanning to characterize tree communities in southern boreal forests *Remote Sens (Basel)*. 2019;**11**:1423. https://doi.org/10.3390/rs11121423.

Zhou T, Zhao C, Wingren CP. *et al.* Forest feature LiDAR SLAM (F2-LSLAM) for backpack systems *ISPRS J Photogramm Remote Sens*. 2024;**212**:96–121. https://doi.org/10.1016/j.isprsjprs.2024.04.025.

Forestry: An International Journal of Forest Research, 2024, 1–13
https://doi.org/10.1093/forestry/cpae058
Original Article